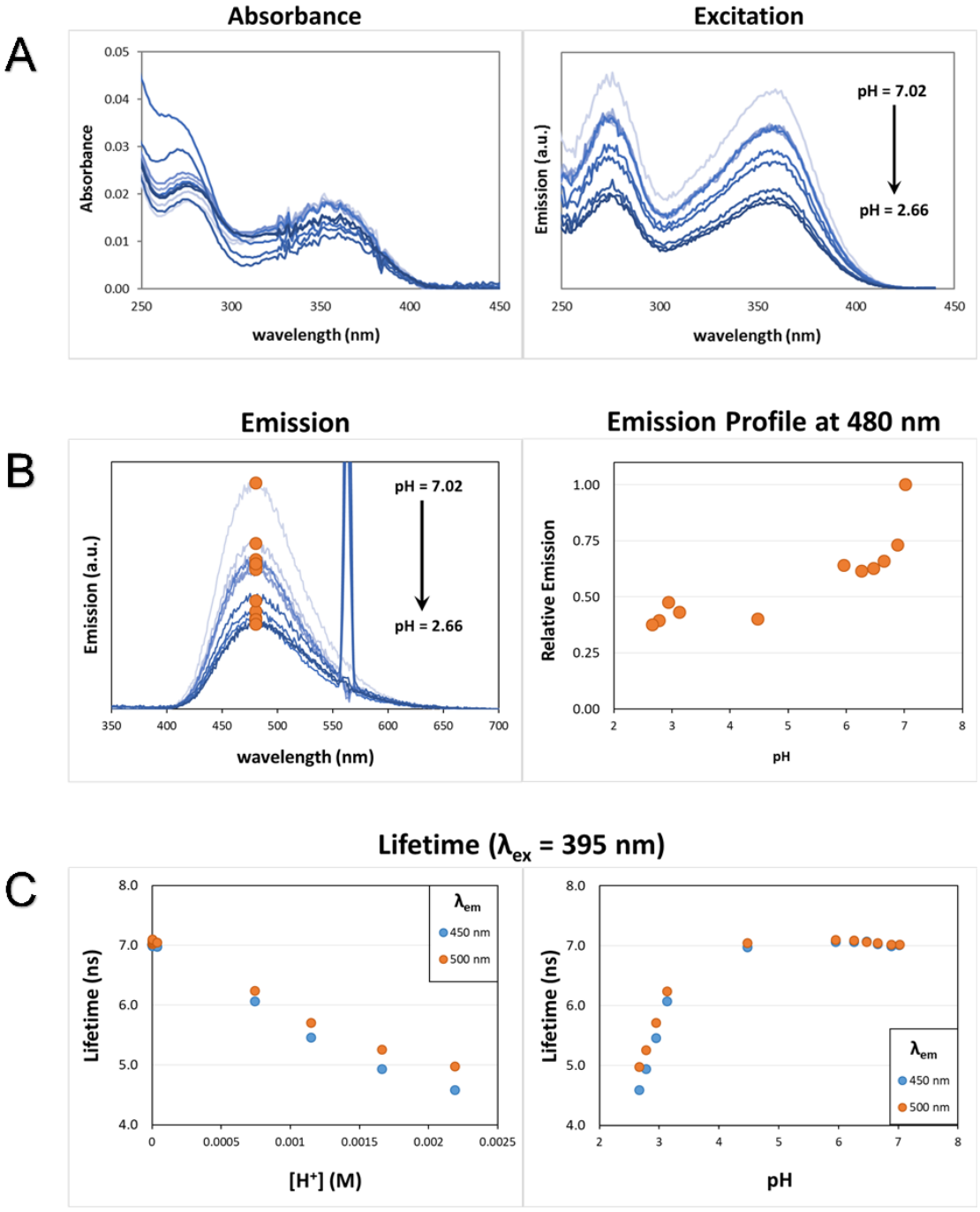

Supplemental Figure 1: pH dependence of rucaparib. All samples were prepared at the same nominal concentration and a digital pH meter was used to determine the pH. (A) The absorbance spectra show weak, random variation with pH, mainly due to the presence of strong scattering in some of the solutions

caused by the neutralization of the buffer with the HCl added. The excitation spectra (λ_{em} = 500 nm) decrease monotonically with decreasing pH. (B) The emission spectra (λ_{em} = 280 nm) also decrease with decreasing pH. Some of these spectra also display a strong Raman scattering peak near 560 nm due to the salts generated upon titration with HCl. The right panel shows the decrease in the fluorescence intensity at λ_{max} = 480 nm with decreasing pH. (C) The lifetimes observed at two different emission wavelengths (450 nm, blue circles, and 500 nm, orange circles) also decreases with decreasing pH, but were relatively constant for biologically relevant pH values. When plotted against the proton concentration, the decrease is linear, suggesting a dynamic association/dissociation mechanism consistent with the protonation of one of the rucaparib nitrogens. The most basic nitrogen in the rucaparib structure is the distal secondary amine. This is therefore the most likely site of protonation, with the photophysical changes being attributed to the strong polarization induced as a result. This is corroborated by the shape of the lifetime vs. pH plot, which indicates that protonation occurs at a pH near 4, corresponding to a pK_a value near 10. This is in the range of values for most secondary amines, including the closely analogous N-methylbenzylamine which has a pK_a = 9.58.

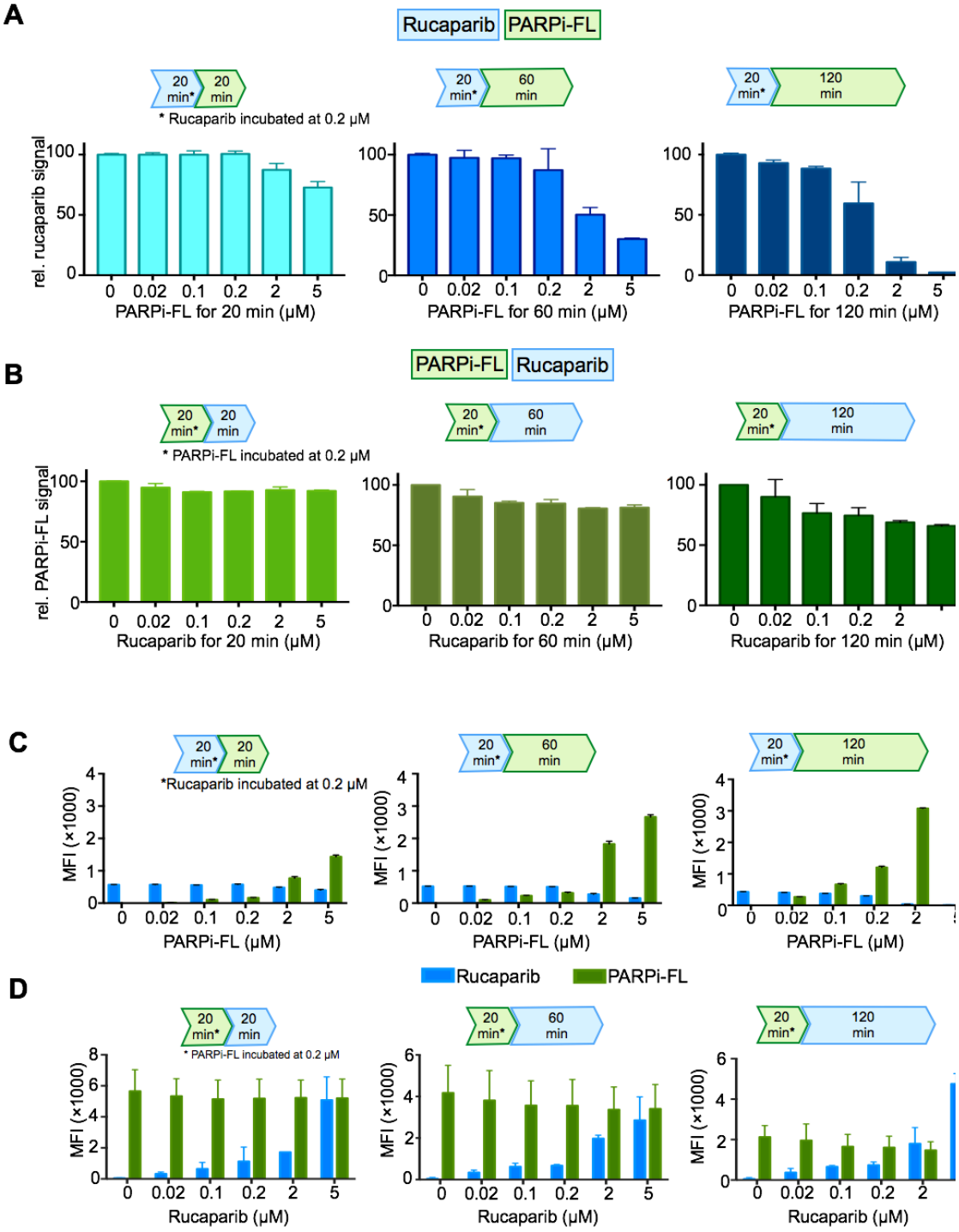

Supplemental Figure 2: Interaction studies. We also investigated how rucaparib and PARPi-FL interacted when incubation with one compound was followed by the other in terms of equilibrium and replacement and report the relative (A, B) and absolute mean fluorescence intensities (C, D) as measured

via flow cytometry. We aimed to determine if interactions between rucaparib and PARPi-FL could have influenced the measurement of the on-target binding time displayed in Figure 4 and to characterize these interactions at higher concentrations and longer incubation times. Therefore, we incubated JHU-LX22 cells first with rucaparib for 20 min at 0.2 uM, followed by PARPi-FL for 20, 60 or 120 minutes at concentrations of 0-5 µM (A, C) (and vice versa– PARPi-FL followed by rucaparib (B, D)). Each incubation step was followed by a 10 minute incubation in fresh media to allow washout of unbound compound. We observed a faster release of rucaparib in presence of PARPi-FL at high PARPi-FL concentrations (2, 5 µM) and longer incubation times (1 hour, 2 hours). At the conditions chosen to determine the on-target binding time of rucaparib, no effects of the presence of PARPi-FL at the concentration of 0.2 µM were observed. For the reversed case we also observed a decrease of the PARPi-FL signal, which was increasingly accelerated at longer incubation times and higher concentrations, but was not influenced at the condition chosen to measure the on-target half-life of rucaparib (0.2 uM, 20 min). Cells were measured on a Fortessa II Flow Cytometer and data were analyzed with the FlowJo software.